

ORIGINAL ARTICLE

Human mediastinal adipose tissue displays certain characteristics of brown fat

L Cheung¹, J Gertow¹, O Werngren¹, L Folkersen¹, N Petrovic², J Nedergaard², A Franco-Cereceda³, P Eriksson¹ and RM Fisher¹

BACKGROUND: The amount of intra-thoracic fat, of which mediastinal adipose tissue comprises the major depot, is related to various cardiometabolic risk factors. Autopsy and imaging studies indicate that the mediastinal depot in adult humans could contain brown adipose tissue (BAT). To gain a better understanding of this intra-thoracic fat depot, we examined possible BAT characteristics of human mediastinal in comparison with subcutaneous adipose tissue.

MATERIALS AND METHODS: Adipose tissue biopsies from thoracic subcutaneous and mediastinal depots were obtained during open-heart surgery from 33 subjects (26 male, 63.7 ± 13.8 years, body mass index 29.3 ± 5.1 kg m⁻²). Microarray analysis was performed on 10 patients and genes of interest confirmed by quantitative PCR (qPCR) in samples from another group of 23 patients. Adipocyte size was determined and uncoupling protein 1 (UCP1) protein expression investigated with immunohistochemistry.

RESULTS: The microarray data showed that a number of BAT-specific genes had significantly higher expression in the mediastinal depot than in the subcutaneous depot. Higher expression of *UCP1* (24-fold, $P < 0.001$) and *PPARGC1A* (1.7-fold, $P = 0.0047$), and lower expression of *SHOX2* (0.12-fold, $P < 0.001$) and *HOXC8* (0.14-fold, $P < 0.001$) in the mediastinal depot was confirmed by qPCR. Gene set enrichment analysis identified two gene sets related to mitochondria, which were significantly more highly expressed in the mediastinal than in the subcutaneous depot ($P < 0.01$). No significant changes in *UCP1* gene expression were observed in the subcutaneous or mediastinal depots following lowering of body temperature during surgery. *UCP1* messenger RNA levels in the mediastinal depot were lower than those in murine BAT and white adipose tissue. In some mediastinal adipose tissue biopsies, a small number of multilocular adipocytes that stained positively for UCP1 were observed. Adipocytes were significantly smaller in the mediastinal than the subcutaneous depot (cross-sectional area 2400 ± 810 versus 3260 ± 980 μm², $P < 0.001$).

CONCLUSIONS: Human mediastinal adipose tissue displays some characteristics of BAT when compared with the subcutaneous depot at microscopic and molecular levels.

Nutrition & Diabetes (2013) 3, e66; doi:10.1038/nutd.2013.6; published online 13 May 2013

Keywords: mediastinal adipose tissue; brown fat; BAT; UCP1; intra-thoracic fat

INTRODUCTION

Mediastinal adipose tissue is situated within the mediastinum, inside the thorax, but outside the pericardium that encloses the heart and accounts for ~70% of total intra-thoracic fat.^{1–3} The nomenclature of this depot is somewhat confusing as it has been variously described as intra-thoracic^{1,4} extra-pericardial mediastinal² and pericardial^{3,5} adipose tissue, but all of these encompass the mediastinal depot studied here. Accumulation of fat in both the mediastinal and epicardial regions is associated with a number of cardiometabolic risk markers.^{3–5} However, these relationships differ between the depots, implying that the different fat depots in the thoracic cavity could have distinct (patho-)physiological functions. For example, the volume of mediastinal but not epicardial adipose tissue was positively and independently associated with plasma triacylglycerol, C-reactive protein and urinary isoprostane concentrations.^{2–4} A number of studies have investigated epicardial adipose tissue, including its cytokine profile⁶ and macrophage infiltration after diet-induced obesity.⁷ However, the molecular and physiological function of other intra-thoracic fat depots, such as mediastinal adipose tissue, remains poorly characterized.

Both recent^{8–12} and earlier studies¹³ have suggested that the mediastinal depot in humans could contain brown adipose tissue (BAT), even in adults. BAT has an important role in energy homeostasis and non-shivering thermogenesis mediated by uncoupling protein 1 (UCP1) that uncouples the mitochondrial respiration from ATP production, thus dissipating heat. BAT and white adipose tissue (WAT) have different morphologies and molecular functions. BAT is usually brown in colour, owing to its high mitochondrial content, and contains multiple, scattered smaller lipid droplets in its adipocytes, whereas WAT is usually yellow in colour and contains one single lipid droplet in its adipocytes.¹⁴

BAT exhibits high and rapid glucose uptake when stimulated by either insulin or noradrenaline (reviewed in Cannon *et al.*¹⁵), and stimulated murine BAT has a high capacity to clear circulating triacylglycerol,¹⁶ demonstrating the high metabolic activity of this adipose tissue. Consequently, BAT-like attributes of the human mediastinal adipose tissue depot could impact upon its metabolic properties. As an enlargement of this depot seems detrimental and BAT could exist in mediastinal fat, a broad survey of its BAT-related characteristics is needed to understand the relationship

¹Department of Medicine, Solna, Karolinska Institutet, Stockholm, Sweden; ²The Wenner-Gren Institute, Stockholm University, Stockholm, Sweden and ³Department of Molecular Medicine and Surgery, Karolinska Institutet, Stockholm, Sweden. Correspondence: Professor RM Fisher, Atherosclerosis Research Unit, Karolinska Institutet, Center for Molecular Medicine, Karolinska University Hospital (L8:03), SE-171 76 Stockholm, Sweden.

E-mail: rachel.fisher@ki.se

Received 18 February 2013; revised 4 April 2013; accepted 7 April 2013

between the two. Therefore, we examined several BAT characteristics, in terms of morphology and molecular markers, of human mediastinal adipose tissue in comparison with subcutaneous adipose tissue.

MATERIALS AND METHODS

Subjects

Subjects were referred for elective open-heart aortic valve surgery at the Cardiothoracic Surgery Unit, Karolinska University Hospital, Stockholm (Table 1). Exclusion criteria included concomitant significant coronary artery disease at the time of inclusion. The study was conducted according to the principles of the Declaration of Helsinki and was approved by the ethics committee of Karolinska Institutet (approval number 2006/784-31/1), and all subjects provided written informed consent. Ten subjects were included for the initial microarray analysis and a further 23 subjects for quantitative PCR (qPCR) confirmation. Another 25 subjects with characteristics similar to those of the main cohort were included for the investigation of adipose tissue at early and late stages of surgery.

Biopsy procedure

Tissue biopsies were obtained at two different time points during surgery: (1) at the beginning of surgery before the initiation of the heart-lung machine (thoracic subcutaneous fat at the sternotomy incision, and intra-thoracic mediastinal fat); and (2) approximately 2–3 h later, towards the end of surgery, after the patient was decannulated (liver, subcutaneous fat and mediastinal fat). Between these two time points, while the patient was connected to the heart-lung machine, body temperature was lowered by 1–2 °C in a controlled manner, and then raised again to normal at the end of surgery. Therefore, all biopsies were taken when body temperature was around 37 °C, but body temperature had been transiently lowered between the collection of the first and second sets of biopsies. Definitions of the different intra-thoracic adipose tissue depots vary,^{1–4} thereby creating confusion in the literature regarding mediastinal fat. In contrast to those studies in which different intra-thoracic fat depots were defined on the basis of imaging techniques, the mediastinal depot studied in the present study was identified by eye, thereby excluding any possibility of depot misclassification. Biopsies were taken outside the pericardium in the anterior mediastinum, close to the diaphragm and below the thymus in a region free of major vessels. Aliquots of samples were either stored overnight in RNA Later (Ambion, Austin, TX, USA) at 4 °C and then at –80 °C until RNA extraction, or instantly snap frozen and subsequently stored at –80 °C until protein extraction, or fixed in formalin.

RNA extraction

Adipose tissue (~200 mg) was homogenized in Lysing Matrix D tubes (MP Biomedicals, Eschwege, Germany). RNA was extracted by phenol-chloroform separation (TRIzol, Invitrogen, Carlsbad, CA, USA) and cleaned up with RNeasy clean-up kit (Qiagen, Hilden, Germany), according to the manufacturer's protocol. RNA concentrations were measured by NanoDrop and RNA qualities were evaluated by BioAnalyzer (Agilent, Waldbronn, Germany). The mean (s.d.) RNA integrity number of samples analysed by microarrays was 6.6 (1.2). Murine adipose tissue (interscapular BAT and inguinal WAT) was collected from 9-week-old outbred Naval Medical Research Institute mice that had been acclimatized to either 30 or 4 °C for 3 weeks and RNA extracted, as described.¹⁷

Microarray

RNA samples from subcutaneous and mediastinal adipose tissue from 10 subjects (see description in Table 1) were analysed with global expression Affymetrix GeneChip Human Exon 1.0 ST microarrays (Affymetrix, Santa Clara, CA, USA). All expression measurements were pre-processed and log₂ transformed using robust multichip average normalization, as implemented in the Affymetrix Power Tools 1.10.2 package apt-probeset-summarize. This normalization includes a step in which the distribution of gene expression levels on individual microarrays are standardized, essentially normalizing the expression levels to the overall messenger RNA (mRNA) levels. All investigations were done on the core set of meta probesets provided by Affymetrix.

Table 1. Patient demographics

	Microarray (n = 10)	qPCR (n = 23)
Gender (M/F)	8/2	18/5
Age (years)	67.1 ± 16.8	62.3 ± 12.5
BMI (kg m ⁻²)	29.4 ± 4.9	29.3 ± 5.3
WHR	0.98 ± 0.1	0.98 ± 0.1
Glucose (mmol l ⁻¹)	5.4 ± 1.4	5.9 ± 1.4
HbA1c (%)	4.9 ± 1	4.8 ± 0.7
TG (mmol l ⁻¹)	1.5 ± 0.9	1.5 ± 1.1
Cholesterol (mmol l ⁻¹)	5.6 ± 1.2	5.2 ± 1.2
HDL-cholesterol (mmol l ⁻¹)	1.5 ± 0.4	1.2 ± 0.5
LDL-cholesterol (mmol l ⁻¹)	3.5 ± 1	3.2 ± 0.9
HsCRP (mg l ⁻¹)	4.6 ± 5.6	2.6 ± 4.4
γ-GT (U l ⁻¹)	36.4 ± 20.2	30.1 ± 31.8

Abbreviations: BMI, body mass index; γ-GT, gamma glutamyl transferase; HbA1c, glycosylated haemoglobin; HDL, high-density lipoprotein; HsCRP, C-reactive protein measured with a high sensitivity method; LDL, low-density lipoprotein; qPCR, quantitative PCR; TG, triacylglycerol; WHR, waist-to-hip ratio. Data are presented as mean ± s.d. There were no significant differences between the two groups for any of the parameters by Student's *t*-test.

Quantitative PCR

RNA samples from a separate group of 23 patients (see description in Table 1) were used for complementary DNA synthesis with SuperScript III (Invitrogen) and analysed with TaqMan gene expression assays (*PPIA*: Hs99999904_m1, *TBP*: Hs00427620_m1, *UCP1*: Hs00222453_m1, *PRDM16*: Hs00223161_m1, *COBL*: Hs00391205_m1, *CIDEA*: Hs00154455_m1, *PPARGC1A*: Hs00222453_m1, *SHOX2*: Hs00243203_m1 and *HOXC8*: Hs00224073_m1; Applied Biosystems, Foster City, CA, USA). A pooled adipose tissue sample was used as an inter-plate control, which was assigned an arbitrary value of 1 and diluted to form a standard curve for each qPCR assay. All individual levels were expressed relative to this control.

To identify a reliable reference gene between depots, the expression levels of *PPIA*, *TBP* and *RPLP0* were analysed with the geNorm algorithm.¹⁸ *PPIA* was found to be the most stable reference gene and the stability of its expression in adipose tissue has been reported previously.¹⁹ The expression level of *PPIA* did not differ between subcutaneous and mediastinal samples, and was not altered as a result of surgery: subcutaneous early 27.9 ± 0.36; subcutaneous late 27.8 ± 0.57; mediastinal early 27.3 ± 0.68; and mediastinal late 27.6 ± 0.58, presented as mean Ct values ± s.d. Therefore, the expression levels of target genes were normalized to that of *PPIA*.

Mouse complementary DNA was prepared as previously described¹⁰ and analysed with TaqMan gene expression assays (*Ucp1*: Mm01244861_m1, *Tbp*: Mm00446971_m1, Applied Biosystems).

Western blot

Frozen human and mouse adipose tissue was ground in a buffer containing 50 mM Tris pH 7.4, 150 mM NaCl, 1% Triton X-100, 1% NP-40, 0.1% SDS, 1 mM phenylmethanesulfonyl fluoride and protease inhibitors with a dounce homogenizer on ice. The lysate was centrifuged to pellet lipids and tissue/cell debris, and then quantified using the bicinchoninic acid (BCA) method (Thermo Scientific, Rockford, IL, USA). Protein (40 µg) was loaded and run on a 15% SDS-polyacrylamide gel and transferred to a polyvinylidene difluoride membrane, blocked with 5% milk, incubated with a primary mouse monoclonal anti-human UCP1 antibody (R&D systems, Minneapolis, MN, USA) at 1:300 dilution overnight and then with a rabbit anti-mouse IgG biotin-conjugated secondary antibody (1:50 000, Vector Laboratories Inc., Burlingame, CA, USA) for 1 h at room temperature. The signal was detected by ECL plus Western Blotting Detection System (GE Healthcare, Buckinghamshire, UK) with Amersham Hyperfilm ECL (GE Healthcare).

Immunohistochemistry

Immunostaining was performed on sections of 5-µm-thick formalin-fixed paraffin-embedded adipose tissue samples using a standard protocol. Serial sections were demasked in DIVA Decloaker (Biacore Medical,

Concord, CA, USA) before incubation overnight at 4 °C with a primary mouse monoclonal anti-human UCP1 antibody (R&D systems) at 1:1000 dilution. A secondary biotinylated goat anti-mouse IgG antibody (1:2000, DakoCytomation, Glostrup, Denmark) was used in combination with avidin–biotin peroxidase complex (Vector Laboratories), followed by 3,3'-diaminobenzidine tetrachloride (Vector Laboratories) for visualization. All sections were counter-stained with filtered Harris hematoxylin (Histolab, Gothenburg, Sweden) and examined with light microscopy.

Adipocyte size measurement

Formalin-fixed paraffin-embedded sections were stained with haematoxylin and mounted on glass for microscopic examination at $\times 20$ magnification. Images were analysed by ImageJ software (rsbweb.nih.gov/ij/) according to the principle described by Chen and Farese.²⁰ In short, the background threshold was set to give the best visualization of adipocyte plasma membranes (usually between 220 and 230). Images were then flattened to binary images. 'Fill hole' function was applied to remove debris and optical artefacts, skeletonizing the membrane. Adipocyte area was 'dilated' and/or 'eroded' in order to optimize the separation of adipocytes graphically. Then the 'watershed' was applied to ensure the correct representation of adipocytes. The area of an average of 240 adipocytes was then measured using the function 'analyse particles' (with parameters: size: 500 μm^2 –50 000 μm^2 , circularity: 0–1.00, exclude on edges).

Statistical analysis

Gene expression data from microarrays were analysed with R-Bioconductor packages (www.bioconductor.org), and Student's *t*-test of paired-sample was performed. Gene set enrichment analysis was performed using the GAGE package for R (2.15.1) comparing subcutaneous and mediastinal adipose tissue. This algorithm tests whether a particular group of genes shows greater differential expression than that which could be expected in a randomly selected group of genes of the same size. The algorithm settings were for group-wise comparison and included both up- and downregulated genes. Adjusted *P*-values (*q*-values) were calculated using the Benjamini and Hochberg step-up false discovery rate-controlling procedure.²¹ For qPCR analysis, gene expression in subcutaneous and mediastinal adipose tissue, and in early versus late stages of surgery was compared using a Wilcoxon signed-rank test. Adipocyte size was analysed with paired two-sample Student's *t*-test. Relationships between variables were analysed by Spearman's rank correlation. Data are presented as mean \pm s.d. unless otherwise stated.

RESULTS

Differential gene expression between mediastinal and subcutaneous adipose tissue depots

Subcutaneous and mediastinal adipose tissue biopsies were obtained from subjects undergoing elective heart surgery (Table 1). The subjects were mainly men in their 60s who were somewhat overweight, but otherwise metabolically healthy. Initially, 10 paired samples of mediastinal and subcutaneous adipose tissue were analysed with global gene expression microarrays. We first compared in the two depots the expression of selected genes that had previously been described as BAT and WAT markers in humans and/or mice, including transcription factors involved in adipocyte differentiation^{9,12,17,22–33} (Table 2).

Out of 18 genes previously described as markers of human BAT, the expression levels of 7 (*IGHG1*, *COBL*, *AGT*, *CKMT2*, *ARG2*, *C4A*, *PPARGC1A*) were significantly higher ($P < 0.05$) in mediastinal than in subcutaneous fat. Of the remaining 11 genes, 6 (*UCP1*, *CKMT1A*, *CYFIP2*, *TGM2*, *HMGCS2*, *DIO2*) showed a tendency ($P < 0.1$) towards higher expression in the mediastinal than in the subcutaneous depot. We also considered genes suggested to discriminate between BAT and WAT in cell/animal models. Of eight such markers of BAT, three genes (*CIDEA*, *PPARA*, *CA3*) were significantly more highly expressed in mediastinal adipose tissue, whereas one (*ZIC1*) tended to be higher in subcutaneous fat. Similarly, of seven such markers of WAT, five genes (*SHOX2*, *HOXC8*, *HOXC9*, *DPT*, *INHBB*) had significantly lower expression levels in the mediastinal

depot, although expression of one (*TCF21*) was significantly higher in this depot.

We selected seven genes from the microarray analysis, *UCP1*, *PPARGC1A*, *COBL*, *CIDEA*, *PRDM16*, *HOXC8* and *SHOX2* (expression patterns of these genes are shown graphically in Supplementary Figure 1) for confirmation in a separate group of 23 patients. *UCP1* is a classic BAT marker gene and the key protein for non-shivering thermogenesis, *PPARGC1A* is an important regulatory gene during brown adipocyte differentiation³⁴ and *PRDM16* is a marker of brown adipocytes of myogenic lineage.³² From the microarrays, expression levels of *COBL* and *CIDEA* were highly significantly greater in the mediastinal compared with the subcutaneous depot (fold changes of ~ 1.5). *COBL* has been previously studied in the context of human BAT,²⁵ and *CIDEA* has been implied as a brown-/white-related gene.³⁵ Therefore, these genes were selected for confirmation. Transcription factors *SHOX2* and *HOXC8* are specific to WAT and are involved in the differentiation of white adipocytes.¹⁷ *HOXC8* is expressed specifically in epididymal, but not in murine inguinal WAT, whereas the pattern is reversed for *SHOX2*³³.

qPCR analysis (Figure 1) confirmed significantly higher expression of *UCP1* and *PPARGC1A*, and significantly lower expression of *SHOX2* and *HOXC8* in the mediastinal versus the subcutaneous depot, and the absence of a difference in *PRDM16* expression between the depots. However, higher expression of *CIDEA* in the mediastinal depot could not be replicated in this independent group of patients, and we were unable to detect expression of *COBL* despite using the same assay as reported previously.²⁵

The expression levels of *UCP1* measured with qPCR were relatively low (with mean Ct values of 37 in the subcutaneous depot and 33 in the mediastinal depot). To confirm that the expression of *UCP1* in adipose tissue was not artefactual, we analysed *UCP1* expression in five human liver samples (which served as negative controls). *UCP1* expression could not be detected in the liver samples (data not shown); therefore, we believe that true *UCP1* expression is detected in the human adipose tissue samples.

UCP1 expression levels in neither the subcutaneous nor the mediastinal depot correlated significantly with any of the clinical parameters included in Table 1.

Mitochondrial gene sets were enriched in the mediastinal depot. To identify gene ontology (GO) gene sets that were significantly enriched in the mediastinal compared with the subcutaneous depot, gene set enrichment analysis was performed. Four such significant gene sets were identified (Figure 2a), two of which were related to mitochondria and represented different GO terms: mitochondrial matrix ($q = 0.002$) and mitochondrial inner membrane ($q = 0.011$). In addition, 3 other mitochondrial related gene sets, mitochondrial respiratory chain complex I ($q = 0.166$), fatty-acid beta oxidation ($q = 0.183$) and mitochondrial nucleoid ($q = 0.183$), were identified within the top 20 enriched gene sets in the mediastinal compared with subcutaneous adipose tissue, although these gene sets did not reach statistical significance. The top 20 GO gene sets enriched in the mediastinal depot are listed in Supplementary Table 1. Volcano plots of the two significantly enriched mitochondrial gene sets are shown in Figures 2b and c and those of all the top 20 enriched gene sets in the mediastinal depot are shown in Supplementary Figure 2.

An acute clinically controlled lowering of body temperature did not change *UCP1* expression

During surgery, the patients' core temperature was lowered by 1–2 °C. Therefore, we investigated whether a clinically controlled lowering of body temperature under anaesthesia could alter *UCP1* expression. We analysed paired adipose tissue biopsies collected from 25 patients before the lowering of body temperature

Table 2. Expression in subcutaneous and mediastinal adipose tissue of selected markers of brown and white fat

Gene name	Mean expression		Fold change	P-value	References	Probe name
	Subcutaneous	Mediastinal				
Potential markers of brown adipose tissue in humans						
<i>UCP1</i>	4.85 ± 0.16	5.60 ± 1.16	1.68	0.07	9,12,23,25	2787073
<i>CKMT1A</i>	4.34 ± 0.12	4.71 ± 0.49	1.30	0.07	25	3591558
<i>KCNK3</i>	6.99 ± 0.12	7.04 ± 0.10	1.03	0.40	25	2473936
<i>IGHG1</i>	7.23 ± 0.21	7.65 ± 0.64	1.33	0.04	25	3581637
<i>COBL</i>	6.85 ± 0.14	7.43 ± 0.49	1.49	0.006	25	3050609
<i>CYFIP2</i>	7.88 ± 0.30	8.26 ± 0.62	1.30	0.07	25	2837266
<i>CYP1A2</i>	7.87 ± 0.16	7.96 ± 0.21	1.07	0.30	25	3601827
<i>MYH11</i>	8.94 ± 0.74	9.07 ± 0.70	1.09	0.60	25	3682028
<i>AGT</i>	8.20 ± 0.42	8.86 ± 0.47	1.58	0.0007	25	2460296
<i>CKMT2</i>	8.02 ± 0.43	8.64 ± 0.86	1.54	0.02	25	2818035
<i>TGM2</i>	9.60 ± 0.41	9.87 ± 0.20	1.21	0.08	25	3905145
<i>ARG2</i>	6.69 ± 0.15	6.91 ± 0.28	1.16	0.02	25	3541383
<i>CA12</i>	7.37 ± 0.33	7.39 ± 0.32	1.01	0.92	25	3628498
<i>HMGCS2</i>	5.92 ± 0.11	6.34 ± 0.62	1.34	0.06	25	2431031
<i>C4A</i>	7.66 ± 0.18	8.38 ± 0.66	1.65	0.007	25	2902958
<i>ITGA8</i>	6.97 ± 0.65	6.77 ± 0.68	0.87	0.45	25	3279313
<i>PPARGC1A</i>	7.63 ± 0.31	8.03 ± 0.53	1.32	0.01	12,23	2763550
<i>DIO2</i>	4.97 ± 0.12	5.11 ± 0.22	1.10	0.09	12	3573870
Markers of brown adipose tissue in animal and cell models						
<i>CIDEA</i>	9.61 ± 0.43	10.20 ± 0.40	1.51	0.0007	30	3779511
<i>PPARA</i>	8.32 ± 0.17	8.58 ± 0.23	1.19	0.002	22,24,33	3948953
<i>CA3</i>	7.54 ± 0.46	8.08 ± 0.75	1.46	0.008	29,33	3105581
<i>ZIC1</i>	5.35 ± 0.32	5.13 ± 0.12	0.86	0.07	24,33	2646818
<i>MEOX2</i>	10.30 ± 0.19	10.40 ± 0.19	1.04	0.21	24,33	3039485
<i>PRDM16</i>	7.84 ± 0.13	7.93 ± 0.17	1.06	0.28	32	2316953
<i>LHX8</i>	5.48 ± 0.20	5.45 ± 0.11	0.98	0.71	24,33	2342475
<i>ELOVL3</i>	6.93 ± 0.43	6.95 ± 0.63	1.01	0.90	22,28	3261532
Markers of white adipose tissue in animal and cell models						
<i>SHOX2</i>	7.83 ± 0.12	7.29 ± 0.25	0.69	2.13E-006	27,33	2702610
<i>HOXC8</i>	8.09 ± 0.31	7.32 ± 0.30	0.58	0.0005	24,27,31	3416353
<i>HOXC9</i>	6.84 ± 0.35	6.35 ± 0.25	0.71	0.004	27,33	3416344
<i>DPT</i>	12.00 ± 0.59	11.70 ± 0.47	0.80	0.01	17,24	2443120
<i>INHBB</i>	9.09 ± 0.23	8.94 ± 0.22	0.90	0.01	17,24	2503257
<i>TCF21</i>	6.28 ± 0.16	6.47 ± 0.20	1.14	0.04	17	2926447
<i>IGFBP3</i>	9.68 ± 0.14	9.71 ± 0.28	1.02	0.67	17,26	3049292

The signal intensity of the probeset corresponding to each gene measured by microarray is presented. Data are presented as mean ± s.d. Fold changes were calculated as $2^{\text{signal}(\text{ms-sc})}$. P-values were calculated with Student's *t*-test of paired samples. Statistically significant differences are accentuated with italic style.

via the heart-lung machine, and again after the patients were decannulated and their body temperature had returned to ~37 °C ($n=25$ for subcutaneous, $n=10$ for mediastinal). No significant change in *UCP1* gene expression was observed in either the subcutaneous (early: 0.55 ± 1.08 , late: 0.73 ± 1.39 arbitrary units, $P=0.240$) or mediastinal depot (early: 1.05 ± 1.00 , late: 0.69 ± 0.39 arbitrary units, $P=0.557$).

As beta blockers have been reported to inhibit the activity of BAT,⁹ we investigated whether *UCP1* expression differed according to medication status. There were no differences in *UCP1* expression in either subcutaneous or mediastinal adipose tissue in either the microarray (4 of 10 patients on beta blockers) or qPCR (12 of 23 patients on beta blockers) groups.

UCP1 expression in human mediastinal adipose tissue is much lower than in murine adipose tissues

To determine how the mRNA levels of *UCP1* in human adipose tissue compare with those in mouse adipose tissues, qPCR was performed on human subcutaneous and mediastinal adipose tissue and on murine brown and white fat, using *TBP* as a common reference gene. *TBP* levels were similar in all tissues (Table 3).

Levels of *UCP1* mRNA in human mediastinal adipose tissue were >1000-fold lower than those of *Ucp1* in murine brown fat, and were even some 30-fold lower than those in murine white fat, as assessed by comparing Ct values (Table 3). We attempted to compare *UCP1* protein levels in mouse and human adipose tissue samples. Western blot analysis revealed a single band in the murine BAT, but no signal was visible in either mouse WAT or human adipose tissue samples (data not shown).

Multilocular adipocytes and positive *UCP1* immunostaining in human mediastinal adipose tissue

As we could consistently quantify *UCP1* mRNA expression in the mediastinal depot, but *UCP1* protein could not be visualized at the whole tissue level using western blot analysis, we proceeded to examine the localization of *UCP1* at the cellular level by immunohistochemistry.

Microscopic examination showed that the tissue morphology was in general rather similar in the two depots (Figures 3a and b). However, the cross-sectional area of adipocytes in the mediastinal depot was significantly less than that in the subcutaneous depot (Figure 3n). Adipocyte size correlated significantly with body mass

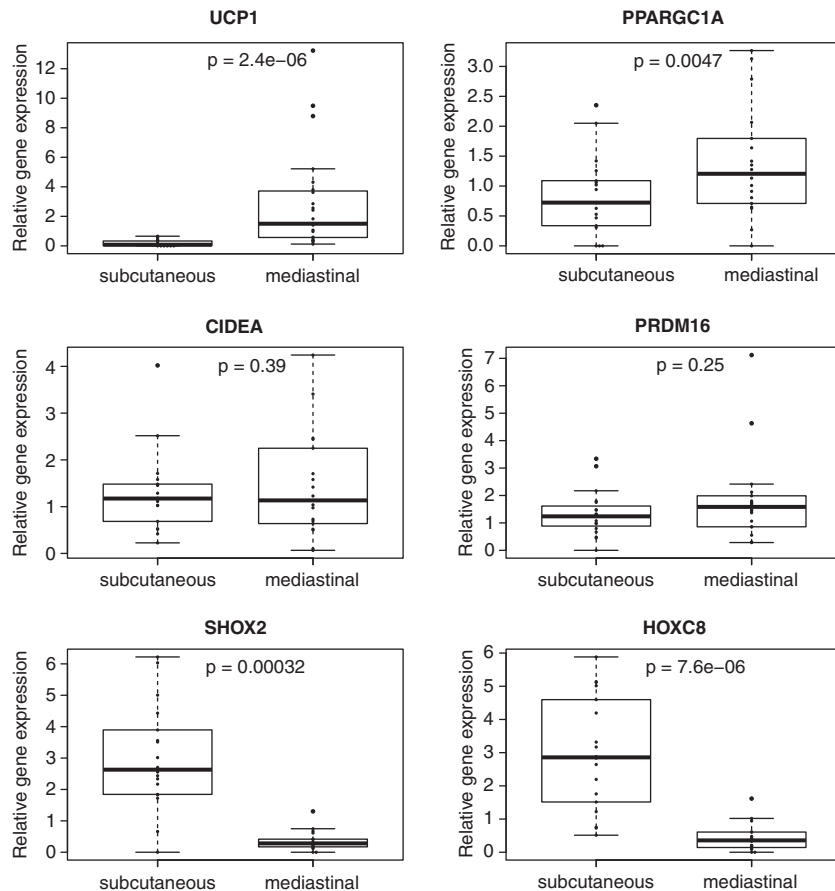


Figure 1. Comparison of gene expression in human subcutaneous and mediastinal adipose tissue. Real-time PCR validation of genes selected from the microarray analysis. Each dot represents one individual ($n = 23$). Box plots represent median (thick black lines), first and third quartiles (outlined boxes), the lowest data point still within 1.5 times the interquartile range from the first quartile (lower whiskers) and the highest data point still within 1.5 times the interquartile range from the third quartile (upper whiskers) of the expression levels of *UCP1*, *PPARGC1A*, *CIDEA*, *PRDM16*, *SHOX2* and *HOXC8* in subcutaneous and mediastinal adipose tissue. Gene expression was normalized to reference gene *PPIA*. *P*-values were calculated according to Wilcoxon paired-sample test.

index in the mediastinal ($r = 0.571$, $P = 0.015$), but not in the subcutaneous depot.

Multilocular lipid droplets were observed in some adipocytes in two out of ten mediastinal adipose tissue biopsies, whereas only unilocular lipid droplets were observed in the adipocytes in the subcutaneous adipose tissue from the same patients (Figures 3c–j). The regions of multilocular adipocytes in these few mediastinal samples were scarce, with the majority of the adipocytes containing unilocular lipid droplets (Figures 3h and j). The regions of mediastinal adipose tissue that contained multilocular lipid droplets stained positively for UCP1 (Figures 3h and j), but weak or no staining for UCP1 was observed in adipocytes containing unilocular lipid droplets in both subcutaneous and mediastinal adipose tissue (Figures 3g–j).

To verify the specificity of the antibody, we tested it on BAT from wild-type and *Ucp1*($-/-$) mice. Marked positive staining was observed in wild-type BAT (Figure 3k), whereas no staining was observed in *Ucp1*($-/-$) BAT (Figure 3l), thereby demonstrating the specificity of this antibody for UCP1.

DISCUSSION

Our findings

We show here that human mediastinal adipose tissue displays some characteristics of BAT when compared with the subcutaneous depot at the microscopic and molecular levels. The

differential gene expression pattern of the mediastinal versus the subcutaneous depot resembled that of BAT versus WAT, and several GO gene sets related to mitochondria were significantly enriched in the mediastinal depot. Moreover, adipocytes in the mediastinal depot were significantly smaller than those in the subcutaneous depot. However, levels of *UCP1* mRNA in mediastinal adipose tissue were much lower than those in murine BAT and were lower even than those in murine WAT. Nonetheless, in a small number of mediastinal biopsies, some adipocytes containing multilocular lipid droplets and demonstrating positive UCP1 immunoreactivity were observed.

Mediastinal adipose tissue displays more BAT characteristics than the subcutaneous depot

Our data reveal a number of differences between human subcutaneous and mediastinal adipose tissue depots. Under thermoneutral conditions, BAT in rodents normally contains a mixture of adipocytes with either unilocular or multilocular lipid droplets and has smaller adipocytes than white fat.¹⁴ Our data showed that adipocytes in the human mediastinal depot were consistently smaller than those in the subcutaneous depot, and that regions of multilocular lipid droplets could be found in a small number of mediastinal samples.

Our data also revealed a consistent BAT gene expression signature in the mediastinal depot. Thirteen of the 18 previously reported markers of human BAT examined here were more highly

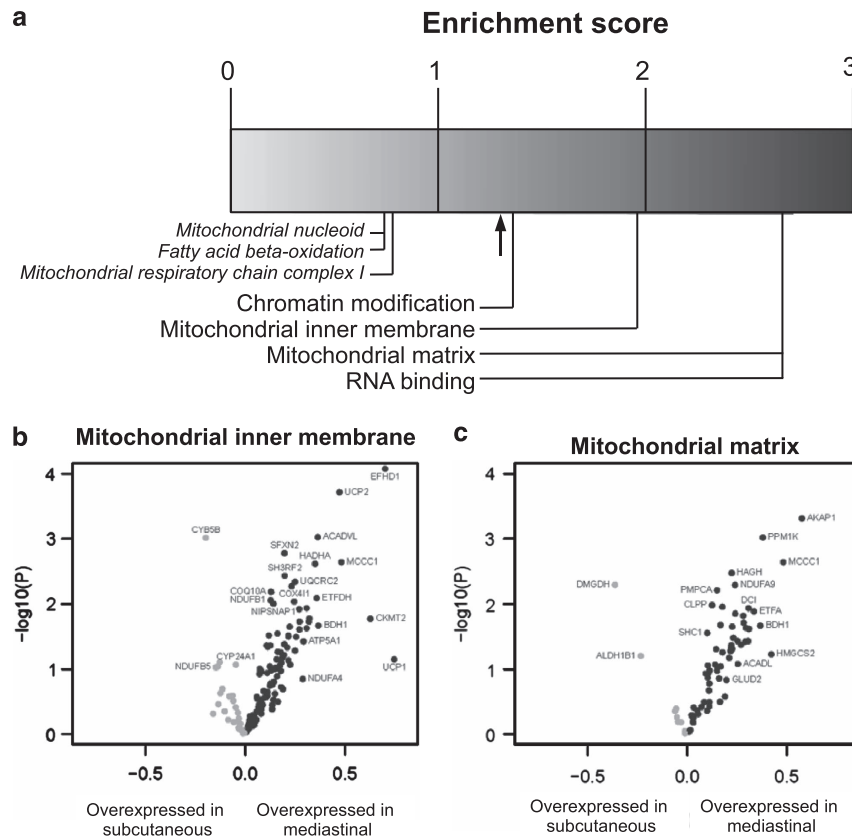


Figure 2. Analysis of gene sets enriched in human subcutaneous versus mediastinal adipose tissue. **(a)** Graphical representation of gene set enrichment score calculated as $-\log(q)$. The arrow indicates a significance level of $q = 0.05$. Gene sets significantly enriched in mediastinal compared with subcutaneous adipose tissue are marked (plain text) at their corresponding enrichment scores. Three additional gene sets within the top 20 enriched gene sets are indicated in italics. **(b)** and **(c)** Volcano plots of genes in the significantly enriched mitochondrial gene sets. Volcano plots of genes in the top 20 GO gene sets enriched in the mediastinal depot are available in Supplementary Figure 2.

Table 3. Comparison of *UCP1* mRNA expression between different depots in human and mouse

Depots	<i>qPCR Ct value</i>		
Human (23 paired samples)	<i>UCP1</i>	<i>TBP</i>	
	Subcutaneous 36.5 ± 1.3	31.7 ± 1.4	
Mediastinal	32.7 ± 1.9	31.1 ± 1.2	
Mouse ($n = 6$ per group)	<i>Ucp1</i>	<i>Tbp</i>	
	Inguinal white (thermoneutral)	27.7 ± 0.8	30.2 ± 0.3
	Brown (thermoneutral)	21.3 ± 0.3	30.5 ± 0.3
	Inguinal white (cold acclimatized)	22.0 ± 0.9	30.6 ± 0.4
	Brown (cold acclimatized)	21.0 ± 4.1	31.2 ± 0.4

The quantitative PCR Ct values of expression assays for *UCP1* and *TBP* in human subcutaneous and mediastinal adipose tissue depots were compared with those of expression assays for *Ucp1* and *Tbp* in mouse white and brown adipose tissue in thermoneutral and cold conditions. Data are presented as mean \pm s.d.

expressed in the mediastinal compared with the subcutaneous depot significantly or as a trend. Of 15 genes shown to discriminate between BAT and WAT in cell or animal models, the differential expression of 8 genes supported the concept that human mediastinal adipose tissue was browner than subcutaneous, but the expression pattern of two genes indicated the opposite. These data might reflect the limitations of taking genes identified as distinguishing between BAT and WAT in cell/animal models and applying them to the human setting.

In addition to confirmation of the *UCP1* microarray data in an independent group of subjects and a significantly higher expression of one of the main regulators of differentiation of brown adipocytes, *PPARGC1A*,³⁴ in the mediastinal depot, we were also able to confirm a significantly higher expression in subcutaneous adipose tissue of two transcription factors (*SHOX2* and *HOXC8*) shown to be specific for mouse WAT.¹⁷ The differential expression of transcription factors regulating white/brown adipogenesis in the two depots suggests that the adipocytes in the mediastinal depot might not be as 'white' as those in the subcutaneous depot, implying that these depots are of different lineages and have different physiological functions. The expression of *PRDM16* was not statistically different in the mediastinal versus the subcutaneous depot, which is in line with previous observations in human mediastinal,³⁶ epicardial^{23,36} and supraclavicular fat.¹²

Gene set enrichment analysis of the entire microarray data identified four GO gene sets that were significantly enriched in the mediastinal compared with the subcutaneous depot, two of which were related to mitochondria. An additional 3 gene sets related to mitochondria appeared within the top 20 enriched gene sets in the mediastinal depot. This over-representation of gene sets related to mitochondria indicates higher mitochondrial activity in the mediastinal depot, which is in line with the other BAT characteristics of mediastinal adipose tissue described above.

The metabolic relevance of BAT in the mediastinum

UCP1 is the classic BAT marker that has been used as the hallmark for identification of BAT. We showed that *UCP1* was expressed at

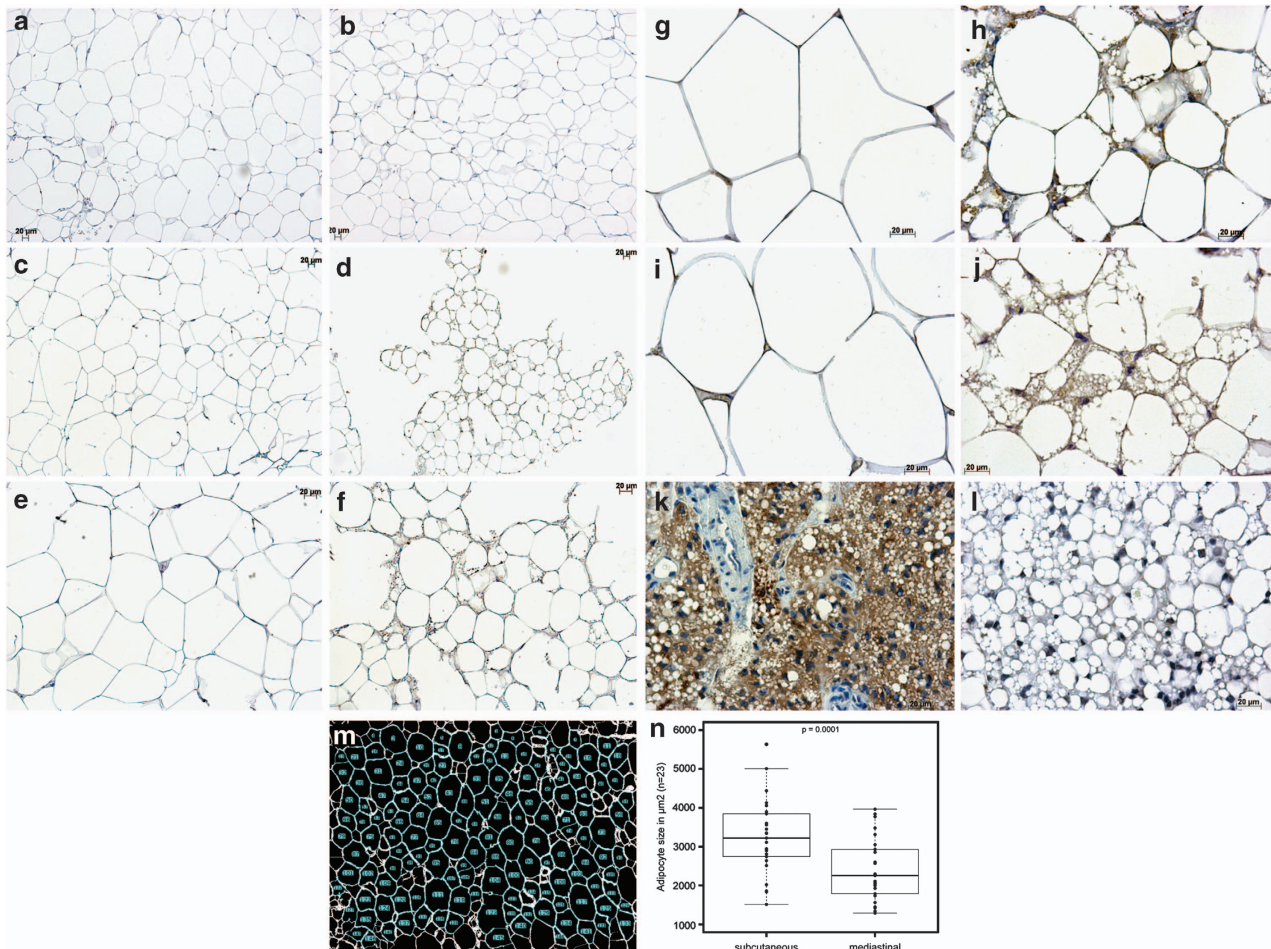


Figure 3. Histochemical analysis of human subcutaneous and mediastinal adipose tissue. Representative microscopic picture of subcutaneous (a) and mediastinal (b) adipose tissue samples from one patient ($\times 10$, stained with haematoxylin). Immunohistochemical staining of UCP1 using primary monoclonal anti-UCP1 antibody at 1:1000 dilution (c–l). Paired subcutaneous (c, e and g) and mediastinal (d, f and h) adipose tissue samples from another patient at $\times 10$ (c and d), $\times 20$ (e and f) and $\times 40$ (g and h) magnification. Paired subcutaneous (i) and mediastinal (j) adipose tissue samples from a third patient at $\times 40$ magnification. BAT from a wild-type (k) and *Ucp1*($-/-$) mouse (l) at $\times 40$ magnification. Counting mask (m) for the determination of adipocyte size from tissue sections at $\times 10$ magnification. (n) Box-plot of adipocyte size (μm^2) from 25 patients with *P*-value of Student's *t*-test with paired samples. Scale bars of $20\ \mu\text{m}$ are shown in a–l.

significantly higher levels in the mediastinal compared with the subcutaneous depot. In mediastinal adipose tissue, *UCP1* was expressed at a reasonably moderate range, with an expression level similar to that of the reference gene *TBP*, but $\sim 100\times$ less than adiponectin (data not shown). Although *UCP1* expression in intra-thoracic fat has been reported previously,^{23,36,37} data on absolute levels of mRNA and protein expression are lacking. Therefore, in order to investigate whether the BAT characteristics of the mediastinal depot were likely to be of physiological and functional significance, we compared *UCP1* gene expression in human and rodent adipose tissue. *UCP1* mRNA levels were >1000 -fold higher in murine BAT as compared with human mediastinal adipose tissue, and even thermoneutral murine WAT expressed *Ucp1* at several-fold higher levels than mediastinal tissue. The higher *UCP1* mRNA levels in human mediastinal compared with subcutaneous adipose tissue might be explained by the presence of a few isolated brown adipocytes in the mediastinal depot. Our analysis supported such a scenario, with a few regions of multilocular adipocytes identified in a small number of mediastinal adipose tissue biopsies. Furthermore, UCP1 protein was detected in the regions of multilocular lipid droplets. This would imply that the amount of UCP1 protein in the mediastinal depot at the tissue level is very low, as supported by

our finding that UCP1 protein was not detectable by western blot in whole tissue extracts. Taken together, our data suggest that the heat-generating potential of human mediastinal adipose tissue in the patient group investigated is not comparable to that of murine BAT. However, given that the present subjects (elderly and overweight) represent a group with very little active BAT in comparison with young and slim individuals, we may have characterized the remainder of active BAT from earlier in life, when the amount may have been more substantial and potentially possessed a metabolic activity that could at least have been of local functional significance. In line with this, we did not find any significant relationships between *UCP1* expression levels in the mediastinal depot and metabolic parameters, supporting the concept that the metabolic significance, at the whole body level, of UCP1 expression in the mediastinum in these subjects is limited.

The existence of so called 'brite' or 'beige' adipocytes within adipose tissue has recently been described, cells of WAT origin that have differentiated into brown adipocytes.²² However, we found no consistent differences in the expression levels of a recently identified set of murine 'beige-selective' genes³⁸ between subcutaneous and mediastinal adipose tissue (data not shown). Therefore, both the developmental perspective (as discussed

above) and our data suggest that mediastinal adipose tissue is more likely to be remnant of BAT than a brite/beige depot.

Although body temperature was transiently lowered slightly (not $<35^{\circ}\text{C}$) during the surgery in the present report, this temperature decrease did not alter *UCP1* gene expression in either mediastinal or thoracic subcutaneous adipose tissue. A probable explanation for this observation is that neurotransmission during anaesthesia is deranged, and therefore an acute clinically controlled lowering of body temperature during anaesthesia is not comparable to a prolonged exposure to a cold ambient temperature. Although we cannot exclude the possibility that we were unable to detect extremely localized changes in *UCP1* expression during the surgery (owing to the impossibility of sampling identical sites at the two time points), we believe this is an unlikely scenario as the RNA was extracted from tissue pieces that represented more than just a very small number of cells.

The amount of intra-thoracic fat has recently been related to cardiovascular diseases including atherosclerosis^{39,40} and associated with many cardiometabolic risk factors.^{1–5} In the present study, we found that human mediastinal adipose tissue displays some BAT characteristics. However, we found no significant relationships between *UCP1* expression in mediastinal adipose tissue and plasma parameters (including high-density lipoprotein, as reported elsewhere³⁶). As the mediastinal depot accounts for $\sim 70\%$ of the total intra-thoracic fat,^{1–3} a greater understanding of the physiological properties of mediastinal fat, such as lipid metabolism and cytokine profiles, is needed.

CONCLUSION

We present novel molecular and microscopic data on human mediastinal adipose tissue. Although the data remain descriptive, we have characterized this depot in comparison with paired subcutaneous samples using a number of different methods, and show that it has several characteristics typical of BAT. We report expression of *UCP1* mRNA in mediastinal adipose tissue from elderly subjects, despite the fact that the prevalence of BAT is higher in younger individuals.^{9,10} Levels of *UCP1* mRNA were far from comparable to those in murine BAT or murine WAT. During the surgery, short-term lowering of body temperature under anaesthesia did not regulate *UCP1* expression. Finally, in some mediastinal adipose tissue biopsies, we observed isolated regions of adipocytes containing multilocular lipid droplets and positive *UCP1* immunoreactivity. Therefore, we suggest that human mediastinal adipose tissue in adults could be a BAT depot, but the physiological and metabolic relevance remains to be studied, particularly in younger adults where the amounts of *UCP1* are likely to be higher, and thus the potential metabolic significance of the tissue could be greater.

CONFLICT OF INTEREST

The authors declare no conflict of interest.

ACKNOWLEDGEMENTS

We gratefully acknowledge the clinical staff at the Cardiothoracic Surgery Unit at the Karolinska University Hospital for their contribution. This study was supported by the Fredrik and Ingrid Thuring foundation, the Novo Nordisk Foundation, the Swedish Diabetes Association and the Swedish Research Council. Some of the authors are members of the EU research group DIABAT.

REFERENCES

- Rosito GA, Massaro JM, Hoffmann U, Ruberg FL, Mahabadi AA, Vasan RS *et al*. Pericardial fat, visceral abdominal fat, cardiovascular disease risk factors, and vascular calcification in a community-based sample. *Circulation* 2008; **117**: 605–613.
- Sironi AM, Petz R, De Marchi D, Buzzigoli E, Ciociaro D, Positano V *et al*. Impact of increased visceral and cardiac fat on cardiometabolic risk and disease. *Diabet Med* 2012; **29**: 622–627.
- Sicari R, Sironi AM, Petz R, Frassi F, Chubuchny V, De Marchi D *et al*. Pericardial rather than epicardial fat is a cardiometabolic risk marker: an MRI vs echo study. *J Am Soc Echocardiogr* 2011; **24**: 1156–1162.
- Tadros TM, Massaro JM, Rosito GA, Hoffmann U, Vasan RS, Larson MG *et al*. Pericardial fat volume correlates with inflammatory markers: the Framingham Heart Study. *Obesity (Silver Spring)* 2010; **18**: 1039–1045.
- Huang G, Wang D, Zeb I, Budoff MJ, Harman SM, Miller V *et al*. Intra-thoracic fat, cardiometabolic risk factors, and subclinical cardiovascular disease in healthy, recently menopausal women screened for the Kronos Early Estrogen Prevention Study (KEEPS). *Atherosclerosis* 2012; **221**: 198–205.
- Chatterjee TK, Stoll LL, Denning GM, Harrelson A, Blomkalns AL, Idelman G *et al*. Proinflammatory phenotype of perivascular adipocytes. *Circ Res* 2009; **104**: 541–549.
- Fitzgibbons TP, Kogan S, Aouadi M, Hendricks GM, Straubhaar J, Czech MP. Similarity of mouse perivascular and brown adipose tissues and their resistance to diet-induced inflammation. *Am J Physiol Heart Circ Physiol* 2011; **301**: H1425–H1437.
- Nedergaard J, Bengtsson T, Cannon B. Unexpected evidence for active brown adipose tissue in adult humans. *Am J Physiol Endocrinol Metab* 2007; **293**: E444–E452.
- Cypess AM, Lehman S, Williams G, Tal I, Rodman D, Goldfine AB *et al*. Identification and importance of brown adipose tissue in adult humans. *N Engl J Med* 2009; **360**: 1509–1517.
- Saito M, Okamatsu-Ogura Y, Matsushita M, Watanabe K, Yoneshiro T, Nio-Kobayashi J *et al*. High incidence of metabolically active brown adipose tissue in healthy adult humans. *Diabetes* 2009; **58**: 1526–1531.
- Van Marken Lichtenbelt WD, Vanhommel JW, Smulders NM, JMAFL Drossaerts, Kemerink GJ, Bouvy ND *et al*. Cold-activated brown adipose tissue in healthy men. *N Engl J Med* 2009; **360**: 1500–1508.
- Virtanen KA, Lidell ME, Orava J, Heglind M, Westergren R, Niemi T *et al*. Functional brown adipose tissue in healthy adults. *N Engl J Med* 2009; **360**: 1518–1525.
- Heaton JM. The distribution of brown adipose tissue in the human. *J Anat* 1972; **112**: 35–39.
- Cinti S. The adipose organ. *Prostaglandins Leukot Essent Fatty Acids* 2005; **73**: 9–15.
- Cannon B, Nedergaard J. Brown adipose tissue: function and physiological significance. *Physiol Rev* 2004; **84**: 277–359.
- Bartelt A, Merkel M, Heeren J. A new, powerful player in lipoprotein metabolism: brown adipose tissue. *J Mol Med* 2012; **90**: 887–893.
- Waldén TB, Hansen IR, Timmons JA, Cannon B, Nedergaard J. Recruited vs. nonrecruited molecular signatures of brown, 'brite,' and white adipose tissues. *Am J Physiol Endocrinol Metab* 2012; **302**: E19–E31.
- Vandesompele J, Preter KD, Pattyn F, Poppe B, Roy NV, Paeppe AD *et al*. Accurate normalization of real-time quantitative RT-PCR data by geometric averaging of multiple internal control genes. *Genome Biol* 2002; **3**: research0034.
- Neville MJ, Collins JM, Gloyn AL, McCarthy MI, Karpe F. Comprehensive human adipose tissue mRNA and microRNA endogenous control selection for quantitative real-time-PCR normalization. *Obesity (Silver Spring)* 2011; **19**: 888–892.
- Chen HC, Farese RV. Determination of adipocyte size by computer image analysis. *J Lipid Res* 2002; **43**: 986–989.
- Benjamini Y, Hochberg Y. Controlling the false discovery rate: a practical and powerful approach to multiple testing. *J Roy Stat Soc Ser B Methodol* 1995; **57**: 289–300.
- Petrovic N, Walden TB, Shabalina IG, Timmons JA, Cannon B, Nedergaard J. Chronic peroxisome proliferator-activated receptor gamma (PPARgamma) activation of epididymally derived white adipocyte cultures reveals a population of thermogenically competent, UCP1-containing adipocytes molecularly distinct from classic brown adipocytes. *J Biol Chem* 2010; **285**: 7153–7164.
- Sacks HS, Fain JN, Holman B, Cheema P, Chary A, Parks F *et al*. Uncoupling protein-1 and related messenger ribonucleic acids in human epicardial and other adipose tissues: epicardial fat functioning as brown fat. *J Clin Endocrinol Metab* 2009; **94**: 3611–3615.
- Timmons JA, Wennmalm K, Larsson O, Walden TB, Lassmann T, Petrovic N *et al*. Myogenic gene expression signature establishes that brown and white adipocytes originate from distinct cell lineages. *Proc Natl Acad Sci USA* 2007; **104**: 4401–4406.
- Svensson P-A, Jernäs M, Sjöholm K, Hoffmann JM, Nilsson BE, Hansson M *et al*. Gene expression in human brown adipose tissue. *Int J Mol Med* 2011; **27**: 227–232.
- Boney CM, Moats-Staats BM, Stiles AD, D'Ercole AJ. Expression of insulin-like growth factor-I (IGF-I) and IGF-binding proteins during adipogenesis. *Endocrinology* 1994; **135**: 1863–1868.

- 27 Gesta S, Blüher M, Yamamoto Y, Norris AW, Berndt J, Kralisch S *et al*. Evidence for a role of developmental genes in the origin of obesity and body fat distribution. *Proc Natl Acad Sci USA* 2006; **103**: 6676–6681.
- 28 Jörgensen JA, Zadavec D, Jacobsson A. Norepinephrine and rosiglitazone synergistically induce Elovl3 expression in brown adipocytes. *Am J Physiol Endocrinol Metab* 2007; **293**: E1159–E1168.
- 29 Lyons GE, Buckingham ME, Tweedie S, Edwards YH. Carbonic anhydrase III, an early mesodermal marker, is expressed in embryonic mouse skeletal muscle and notochord. *Development* 1991; **111**: 233–244.
- 30 Rong JX, Qiu Y, Hansen MK, Zhu L, Zhang V, Xie M *et al*. Adipose mitochondrial biogenesis is suppressed in db/db and high-fat diet-fed mice and improved by rosiglitazone. *Diabetes* 2007; **56**: 1751–1760.
- 31 Tchkonja T, Lenburg M, Thomou T, Giorgadze N, Frampton G, Pirtskhalava T *et al*. Identification of depot-specific human fat cell progenitors through distinct expression profiles and developmental gene patterns. *Am J Physiol Endocrinol Metab* 2007; **292**: E298–E307.
- 32 Seale P, Kajimura S, Yang W, Chin S, Rohas LM, Uldry M *et al*. Transcriptional control of brown fat determination by PRDM16. *Cell Metab* 2007; **6**: 38–54.
- 33 Walden TB, Timmons JA, Keller P, Nedergaard J, Cannon B. Distinct expression of muscle-specific microRNAs (myomirs) in brown adipocytes. *J Cell Physiol* 2009; **218**: 444–449.
- 34 Petrovic N, Shabalina IG, Timmons JA, Cannon B, Nedergaard J. Thermogenically competent nonadrenergic recruitment in brown preadipocytes by a PPAR{gamma} agonist. *Am J Physiol Endocrinol Metab* 2008; **295**: E287–E296.
- 35 Nordström EA, Rydén M, Backlund EC, Dahlman I, Kaaman M, Blomqvist L *et al*. A human-specific role of cell death-inducing DFFA (DNA fragmentation factor-alpha)-like effector A (CIDEA) in adipocyte lipolysis and obesity. *Diabetes* 2005; **54**: 1726–1734.
- 36 Chechi K, Blanchard P-G, Mathieu P, Deshaies Y, Richard D. Brown fat like gene expression in the epicardial fat depot correlates with circulating HDL-cholesterol and triglycerides in patients with coronary artery disease. *Int J Cardiol*. e-pub ahead of print 22 June 2012; <http://dx.doi.org/10.1016/j.ijcard.2012.06.008>.
- 37 Fain JN, Sacks HS, Bahouth SW, Tichansky DS, Madan AK, Cheema PS. Human epicardial adipokine messenger RNAs: comparisons of their expression in sub-sternal, subcutaneous, and omental fat. *Metabolism* 2010; **59**: 1379–1386.
- 38 Wu J, Sparks LM, Ye L, Choi JH, Giang AH, Khandekar M *et al*. Beige adipocytes are a distinct type of thermogenic fat cell in mouse and human. *Cell* 2012; **150**: 366–376.
- 39 Iacobellis G, Corradi D, Sharma AM. Epicardial adipose tissue: anatomic, biomolecular and clinical relationships with the heart. *Nat Clin Pract Cardiovasc Med* 2005; **2**: 536–543.
- 40 Fantuzzi G, Mazzone T. Adipose tissue and atherosclerosis. *Arterioscler Thromb Vasc Biol* 2007; **27**: 996–1003.



This work is licensed under a Creative Commons Attribution-NonCommercial-NoDerivs 3.0 Unported License. To view a copy of this license, visit <http://creativecommons.org/licenses/by-nc-nd/3.0/>

Supplementary Information accompanies this paper on the Nutrition & Diabetes website (<http://www.nature.com/nutd>)